

Analysis of LBT LINC-NIRVANA simulated images of galaxies

Paolo Ciliegi^a, Andrea La Camera^b, Carmelo Arcidiacono^c, Mario Bertero^b, Patrizia Boccacci^b,
Emiliano Diolaiti^a, Italo Foppiani^d, Matteo Lombini^a, Laura Schreiber^a

^aINAF - Astronomical Observatory Bologna, Via Ranzani 1, 40127, Bologna, Italy

^bDISI, Genova University, Via Dodecaneso 35, 16146, Genova, Italy

^cINAF - Astronomical Observatory Arcetri, L.go E. Fermi 5, 50125, Firenze Italy

^dBologna University - Department of Astronomy, Via Ranzani 1, 40127, Bologna, Italy

ABSTRACT

LINC-NIRVANA (LN) is a Fizeau interferometer that will provide coherent images in the near-IR combining the beams from the two Large Binocular Telescope (LBT) arms, by adopting a Multi-Conjugate Adaptive Optics system (MCAO) that allows for atmospheric turbulence compensation. We applied the software AIRY-LN for the simulation and the reconstruction of LN images in order to investigate the dependence of the image quality from the magnitude of the star used for the PSF extraction. A good knowledge of this dependence is a crucial point for the LN observations, especially for the extragalactic target where the presence of a bright psf-star within the LN field of view of 10×10 arcsec is not granted. Our results, although still preliminary, show that while from the morphological point of view the use of psf-star up to a magnitude of 18 is still acceptable, from the photometric point of view the use of psf-star fainter than $K_s \sim 16$ mag could cause considerable problems.

Keywords: Image simulations, galaxies

1. INTRODUCTION

The Large Binocular Telescope (LBT, Hill and Salinari¹) currently operating on Mount Graham in Arizona with its two 8.4 m mirrors, is an ambitious and innovative undertaking to construct one of the world's largest optical and infrared telescopes. LINC-NIRVANA (LN) (Herbst et al.², Bizenberger et al.³) is a near-infrared image-plane beam combiner with Multi-Conjugate Adaptive Optics system (MCAO), allowing for atmospheric turbulence compensation. The MCAO systems aboard each LBT arm use the light of wavelength $0.6 < \lambda < 1.0 \mu\text{m}$ for wavefront sensing, while the science observations are performed in the wavelength range $1.0 < \lambda < 2.4 \mu\text{m}$, i.e. the range including the J, H and K bands. The fringe tracking, i.e. the measurement of the optical path difference between the two LBT arms, is performed in the near infrared as well.

The performance of the LN interferometer is expected to be very close to the diffraction limit. Due to the binocular nature of the instrument, the Point Spread Function (PSF) may be described as the diffraction limited pattern of an 8.4 m telescope crossed by the fringes due to the interference between the two apertures, characterized by a maximum baseline of approximately 22.8 m. For this reason, the raw images obtained with LN will have an anisotropic angular resolution: typical of an 8 meter class telescope in one axis, approximately 3 times better in the orthogonal axis. The maximum resolution, in the direction of the maximum baseline, ranges from approximately 0.01 arcsec in the J band to 0.02 arcsec in the K band. If exposures are taken at different hour angles in order to obtain a better uv-coverage, an aperture synthesis image reconstruction procedure can provide reconstructed images with the full angular resolution of a 22.8 m single-dish telescope.

The scientific camera is a 2048×2048 infrared array inside a cryostat. The camera optics have a fixed focal length, corresponding to a plate scale of 0.005 arcsec/pixel, which allows to sample the PSF at the Nyquist limit in all conditions. The science field of view is therefore 10×10 arcsec. The technical field of view is larger. The fringe tracker has in fact a field of view of 1×1.5 arcmin.

Here we will present the simulation and the reconstruction of LN images of a relatively distant galaxy at redshift ~ 1 . Different reconstruction methods have been considered in order to test the quality of the reconstruction as function of the method used to extract the PSF from the image and of the magnitude of the PSF star.

2. SIMULATION

2.1 Raw input data : Description and Preparation

To test the very high angular resolution of LN in the observations of relatively distant galaxies we have simulated an observation of a galaxy at $z\sim 1$. To do this, we have generated a synthetic image of a $z\sim 1$ galaxy starting from a real high resolution image of a galaxy at $z\sim 0.1$ obtained with the Hubble Space Telescope (HST). In this way we were able to study all the relevant parameters on the initial “real” low redshift image and then repeat the analysis on the same galaxy “moved” to $z\sim 1.0$ and “observed” with LN.

In order to simulate the expected emission from a galaxy at redshift about 1, the galaxy at $z\sim 0.1$ in the original image with a dimension of ~ 7 arcsec has been scaled down to a dimension of ~ 1 arcsec according to the canonical angular size-distance relationship, while the pixel scale of the image was changed to 5 mas/pixel to match the LN resolution.

Finally, a star for the PSF extraction (psf-star) has been added to the image at a distance of 724 pixels (3.62 arcsec) from the centre of the galaxy (coincident with the image centre). The simulated images at $z\sim 1$ is reported in Fig. 1.

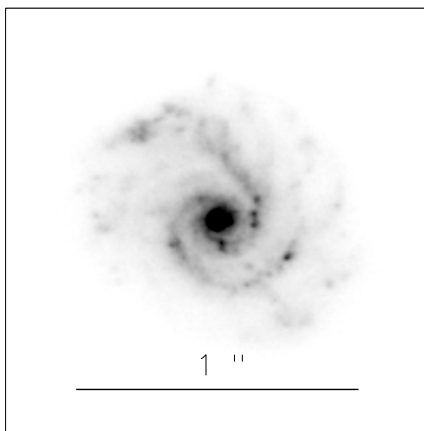


Figure 1. *Simulated galaxy at $z\sim 1$ obtained scaling down the galaxy at $z\sim 0.1$ to a dimension of ~ 1 arcsec and changing the pixel scale from 50 to 5 mas/pixel.*

2.2 Description of Simulated Observing

For all the cases studied in this paper, we assumed that a total of three images at different equispaced hour angles (0, 60 and 120 degrees) have been obtained. Each single image has been obtained assuming an integration time of 60 minutes, for a total integration time of 3 hours. An average K-band sky brightness of 13.5 mag/arcsec² has been assumed as background emission.

Finally, in order to test the sensitivity of the quality reconstruction to the target magnitude and to the psf-star brightness, we considered three different magnitudes (K_s=14, 16 and 18) both for the galaxy and for the psf-star.

2.3 Simulation of Observing Condition (PSF)

The PSFs used in our study have been generated using the software LOST (Arcidiacono et al.⁴). LOST is a numerical tool implemented for the simulation of Multi-conjugate Adaptive Optics (MCAO) systems following the Layer Oriented approach. In particular this code is the one used to perform the numerical simulations of the two LN Adaptive Optics Systems with the Multiple Field of View (MFoV) MCAO technique (Ragazzoni et al.⁵). This code was used both in the design phase of the instrument and in the science case studies currently ongoing.

We implemented several ad-hoc routines to complete the code in order to take into account different rotation angles and airmasses, and to include the effect of the polychromatism on the PSF. In fact LOST computes PSFs which are purely monochromatic: in order to simulate the effect of different wavelengths we applied the reasonable approximation of piling up on a single array different copies of the same monochromatic PSF, scaled in terms of platescale according to the wavelength. This approximation is valid within the three main filters (J, H and Ks), but it is not to go from one to the others.

3. EXPOSURE CONSTRUCTION AND DECONVOLUTION

The construction of the exposures corresponding to the galaxy model and the three orientation angles has been performed using the software package AIRY (Astronomical Image Restoration in interferometrY), version 4.0, available at the URL <http://www.airyproject.eu>. A description of the structure of the package, which is modular, based on IDL and designed to be used together with the CAOS (Code for Adaptive Optics Systems) Application Builder (see Fini et al.⁶), is given in Correira et al.⁷

3.1 Image simulation

A simulation project, for a given object and given hour angles, consists of a number of steps that we outline in this section with reference to our specific problem. For each step we indicate the module of AIRY that must be used.

First the user must provide the hour angles of the observations and the object, as well as the observation band, the magnitude of the object, the pixel size and the total dimension of the object in pixels (in our case 2048×2048 , corresponding to the 10 arcsec FoV of the detector).

Next, one must provide a stack of PSFs, one for each hour angle, all with vertical fringes and use the module RTI (RoTate Image) of AIRY to generate a stack of rotated objects corresponding to the rotation angles given in the previous step. However, the rotation can generate artifacts, in particular in the case of point objects/stars. For this reason we decided to keep the object fixed and rotate the PSFs, working in Fourier space.

The subsequent step is convolution. In general, the input of the module CNV (CoNVolution) consists of the stack of the PSFs and the stack of rotated objects. However, in our case the input is a stack of rotated PSFs and one object. Additional parameters that must be provided are: telescope aperture, integration times for the different angles, total efficiency. The output is a stack of noise-free images.

Finally, the module ADN (ADd Noise) must be used to corrupt the images with background, photon noise and read out noise (RON); the user must provide the magnitude of the background and the σ of the RON. It is also possible to add dark current and saturation. The output is a stack of simulated LINC-NIRVANA images corresponding to the given object.

The procedure we have outlined has been used for generating three stacks of three images (corresponding to three equispaced hour angles), one stack for each value of the common magnitude of galaxy and star.

3.2 Image Reconstruction

The image reconstruction has been performed using modules of the software package AIRY-LN, a numerical tool for deconvolution of images from LINC-NIRVANA. A detailed description of AIRY-LN is reported in Desiderá et al.⁸. The basic algorithm used in our simulation study is described in Bertero & Boccacci⁹ and denoted OSEM (Ordered Subset Expectation Maximization); it was introduced in tomography by Hudson & Larkin¹⁰. This algorithm is essentially an accelerated version of the Richardson-Lucy method (RLM) and has been subsequently modified to compensate for both object rotation and boundary effects (La Camera et al.¹¹).

A generic reconstruction project consists of the following steps.

1. Provide a stack of images with the corresponding hour angles. It is also possible to provide a stack of corresponding PSFs (with vertical fringes) to be used for deconvolution in place of the stack of PSFs of step 3 below. If the PSFs coincide with those used for convolution, the deconvolution based on these PSFs is what we call *Inverse Crime*.

2. Use a rotation functionality, contained in the module LPP (Ln PreProcessing) of AIRY-LN, for de-rotating the images provided in step 1.
3. Use the module LEX (Ln EXtraction - Target/PSF) of AIRY-LN for extracting and extrapolating the PSF from one or more stars in the FoV of the de-rotated images. The result is a stack of de-rotated PSFs. In the version of LEX, used for this study, the extrapolation is performed in terms of a Moffat function with exponent β , $I(r) = a/(b + r^2)^\beta$, which is more general than the Lorentz function ($\beta = 1$) used in La Camera et al.¹¹.
4. Use the module LMD (Ln Multiple Deconvolution) for reconstructing the object. The input consists of two stacks, one of images and one of PSFs; the output is the reconstructed object. The number of iterations is an additional parameter that must be provided by the user.

In our study we do not perform step 2 because, as explained in the previous subsection we generate de-rotated images by de-rotating the PSFs before convolution.

The purpose of our study is to compare the results obtained with three different stacks of PSFs, described below. In all cases the PSFs are normalized to unit volume.

- The PSFs used in the generation of the images (*Inverse Crime*); the purpose is to obtain the best reconstruction allowed by the available images. In this case we must perform only step 1 and step 4.
- The PSFs obtained by extracting the PSFs in a circle centered on the psf-star and then extending it to the full image domain with a zero padding. Two extraction regions are considered around the centroid of the star image: the first with radius 50 pixels and the second with radius 150 pixels.
- The PSFs obtained by extracting the images of the psf-star (as above) and extrapolating the result by means of Moffat functions (see La Camera et al.¹¹ for more details). Different values of β (1.00, 1.10, 1.15, 1.20) have been tested, searching for the value providing the best reconstruction in the sense specified in the next section.

4. ANALYSIS OF RECONSTRUCTED IMAGES OBTAINED USING DIFFERENT METHODS

A first comparison of the quality of the reconstructed images is performed by computing the relative r.m.s. error of the reconstruction with respect to the object used for generating the images. This error is computed only on a region 512×512 containing the galaxy and is defined by

$$\tilde{\rho} = \frac{\|\tilde{f} - f\|}{\|f\|} \quad (1)$$

where f is the original target, \tilde{f} the reconstructed one and $\|f\|$ denotes the ℓ_2 -norm of the array f . We call this quantity the *reconstruction error*.

4.1 Inverse Crime

Since we consider the same galaxy with three different integrated magnitudes: 14, 16 and 18, the inverse crime provides three different reconstructions, with increasing reconstruction error for increasing magnitude. In Figure 2 we give, in the left panel, the reconstruction error vs the number of iterations of the OSEM algorithm while, in the right panel, we report the total flux as a function of the aperture radii for the original galaxy (solid black line), for the coadded image obtained by adding the single exposures without a reconstruction process applied (dot dot dot dashed gray line) and for the reconstructed images obtained with the Inverse Crime technique after 400 iterations (dashed dark gray) and after 1000 iterations (dot line).

The minimum reconstruction error (left panel Figure 2) is 6.3 % for $m=14$, 9.8 % for $m=16$ and 16.7 % for $m=18$. The number of iterations required for reaching this minimum is decreasing for increasing m (>1500 , 700,

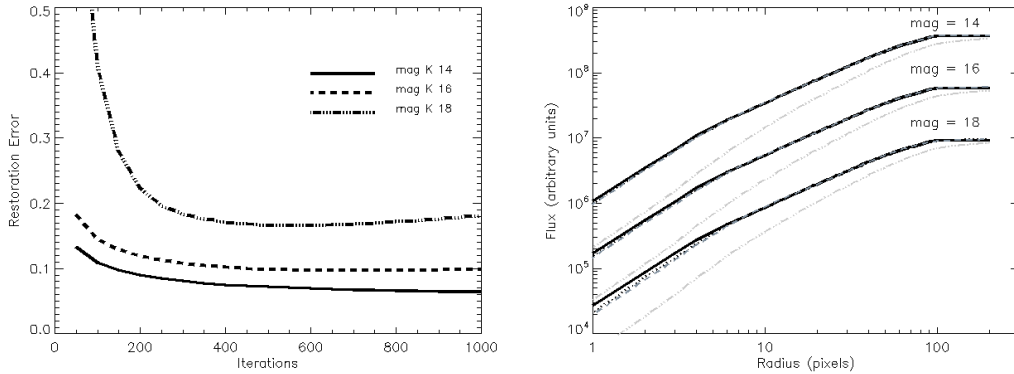


Figure 2. **Left:** The reconstruction error as a function of the number of iterations of the OSEM algorithm for the three different magnitude considered. **Right:** The total flux as a function of the aperture radii for the original galaxy (solid black line), for the non-reconstructed image (dot dot dot dashed gray line) and for the reconstructed images obtained with the Inverse Crime technique after 400 iterations (dashed dark gray) and after 1000 iterations (dot line).

550). In all cases the computation time is of the order of several hours, since we are deconvolving 2048×2048 images. Therefore it should be interesting to estimate the gain in computation time provided by the accelerated algorithms discussed in La Camera et al.¹¹.

From right panel of Figure 2, it is evident that the galaxy flux measured in the Inverse Crime reconstructed images is in very good agreement with the original flux already after 400 iterations, while in the non reconstructed image a large fraction of the galaxy flux is spread in the outer regions of the images, making the photometric accuracy very poor.

4.2 Reconstruction with extracted PSF

The next step towards a more realistic simulation is the reconstruction of the image using a PSF extracted from a point source present in the field of view. Since the reconstruction software requires a PSF on the full image domain, the simplest way to do that is to extract PSFs in a circle centered on an isolated star and then extending them to the full image domain with a zero padding. To do that, we added in our simulated image a star at a distance 3.62 arcsec from the galaxy centre.

Several factors influence the choice of the extraction radius, the most important of which are the imaging crowding and the magnitude of the psf-star (faint psf-stars quickly lose the seeing limited halo in the sky background). We considered two different extraction regions around the centroid of the star image: the first one with radius 50 pixels (0.25 arcsec) and the second one with radius 150 pixels (0.75 arcsec). In Figure 3 (left panel) we show a comparison between the total flux of the original galaxy (magnitude Ks=16, solid black line) and the total flux calculated on the reconstructed images (after 800 iterations) obtained extracting the PSF from a psf-star of magnitude Ks=14 and using a circle of 50 pixels radius (dashed, gray line) and 150 pixels radius (dot dot dot dashed, dark gray line).

As clearly shown in the figure, the extraction of the PSF from a relatively small region around the psf-star and the extension to the full image domain with a zero padding gives very poor results in terms of photometric accuracy. About the 10 % of the total flux of the simulated galaxy has not been reconstructed. This result is what is expected from to the crude approximation of the seeing limited halo of the PSF with a zero padding. It is therefore fundamental, especially in scientific projects demanding a good photometry, to use a better representation of the PSF in the reconstruction process, extracting the PSF from a relatively small region and then extrapolating it to the full image domain with a function that gives a good fit of the faint seeing limited halo. In the next section we will tackle this problem, making a comparison of the total flux and the surface brightness profile between the original target and several images reconstructed with PSF extrapolated with different parameters.

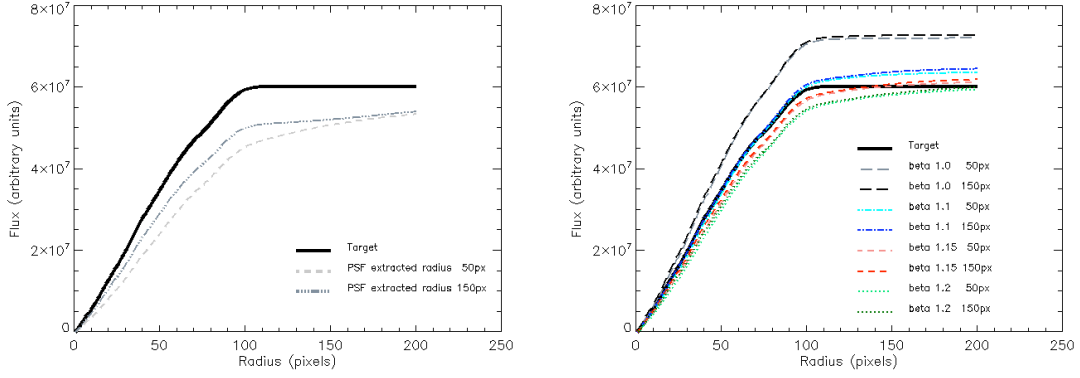


Figure 3. **Left:** The total flux of the original galaxy (magnitude $K_s=16$, solid black line) and the total flux calculated on the reconstructed images (after 800 iterations) obtained extracting the PSF from a psf-star of magnitude $K_s=14$ and using a circle of 50 pixels radius (dashed, gray line) and 150 pixels radius (dot dot dot dashed, dark gray line). The PSFs are extended by zero padding to the full domain. **Right:** The total flux of the original galaxy (magnitude $K_s=16$, solid black line) and the total flux calculated on the reconstructed images (after 1000 iterations) obtained extracting the PSF from a psf-star of magnitude $K_s=14$ and using different radius (50 and 150 pixels) for the extraction region and different β (1.0, 1.1, 1.15 and 1.2) for the Moffat function used to extrapolate to PSF to the full image domain. See text for more details.

4.3 Reconstruction with extracted and extrapolated PSF

In the previous section we showed that the use of the PSF extracted in a small region and extrapolated to the full image domain with a zero padding gives unreliable results in terms of photometric accuracy. Since in the real images it will be impossible to make a fit to the PSF over large region (contamination from the galaxy's halo, crowding in stellar fields like globular clusters, background contamination) a possible way to resolve this problem is to extract the PSF from a small region and then to use a function for the extrapolation to the full image domain. In the left panel of Figure 4 we show the profile of the LN PSF over the full image domain obtained with the software LOST (see section 2.3). The profile is dominated by the adaptive optics core up to a radius of 150 - 200 pixels followed by a rapid decline towards the seeing limited halo. This latter part can be reasonably approximated with a Moffat function in the form $I(r) = a/(b + r^2)^\beta$.

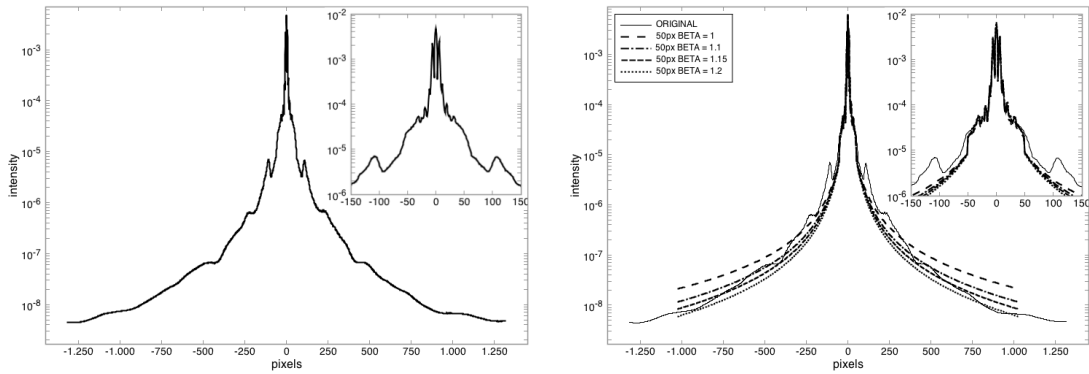


Figure 4. **Left:** The simulated LN PSF profile over the whole image domain obtained with the software LOST. **Right:** The simulated LN PSF profile over the whole image domain with superimposed different PSF profiles obtained extracting the PSF from a circle of radius 50 pixel centred on the psf-star and then extrapolating the profile to the full image domain using a Moffat function with different values of the β parameter.

In the right panel of Figure 4, we show different PSF profiles obtained extracting the PSF from a circle of radius 50 pixel centred on the psf-star and then extrapolating the profile to the full image domain using a Moffat

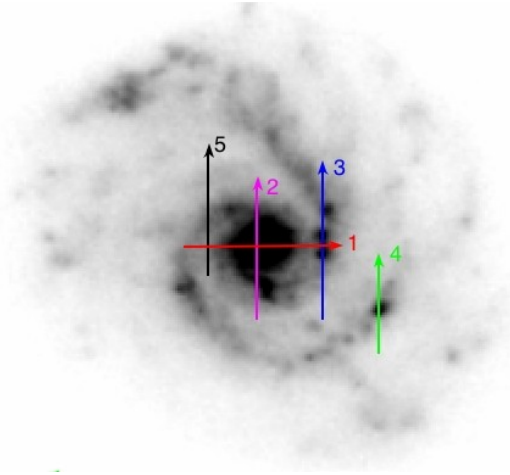


Figure 5. *Simulated galaxy at $z\sim 1$ with superimposed the location of the five slices used to study the reconstruction of the galaxy morphology .*

function with different values of the β parameter. Using different β values (1.0,1.1,1.15 and 1.2) and different aperture to extract the PSF core (50 and 150 pixels radius) we obtained a total of eight different PSFs used for the image reconstruction. A comparison between the total flux as a function of the aperture radii for the original image and for the eight images reconstructed with different PSF is reported in the right panel of Figure 3.

As shown in the figure, the value of $\beta=1.0$ overestimates the total flux of the galaxy at any radius, while the values $\beta=1.2$ underestimates the total flux. The total flux of the galaxy is better reproduced using $\beta = 1.1$ and 1.15. In particular, with $\beta = 1.1$ the reconstructed flux is coincident with the original flux distribution over the whole galaxy size (corresponding to a radius of 100 pixels, 0.5 arcsec). The beta = 1.1 value gives also one of the best fit of the PSF halo (Figure 4). However, in order to chose the best β value, we studied also the morphological reconstruction of the galaxy, analyzing the light distribution in five different slices placed in different region of the galaxy (central core, bright regions in the spiral arms, ecc). The location of the five slices is shown in Figure 5 while in Figure 6 we report the results of our analysis with the light distribution from original galaxy (mag Ks=16) compared with that from the reconstructed images obtained with different values of β (1.1,1.15,1.2) and different aperture for the PSF core extraction (50 and 150 pixels radius centred on a star of mag Ks=14).

From the analysis of Figure 6 it is evident that also from the morphological point of view, the values of $\beta=1.1$ represents the best choice. Therefore in the next section we will use the LN PSF extrapolated with a Moffat function with $\beta=1.1$ to study the quality of the reconstructions as a function of the magnitude of the PSF star used. However, these results on the best functions and parameters for the extrapolation of the LN PSF over the full image domain are very preliminary and more specific simulations (with different scientific targets and/or with different atmospheric conditions) are needed to obtain more robust results.

4.4 Dependency on the psf star brightness

In the simulations presented in this section we tested the quality of the reconstructed image as a function of the magnitude of the psf-star. A good knowledge of this dependence is a crucial point for the LN observations, especially for the extragalactic target where the presence of a bright psf-star within the LN field of view of 10×10 arcsec is not granted. Two different magnitudes have been assumed for the target galaxy (Ks=16 and Ks=18 mag) while for the star used to extract the PSF three different magnitude have been considered (Ks=14, 16 and 18 mag). The PSF have been extracted from a circle of 150 pixels radius for the psf-star with Ks=14 mag and from a circle of 50 pixels radius for the psf-stars with Ks=16 and 18 mag. Finally, all the extracted PSF have been extrapolated to the full image domain using a Moffat function with $\beta=1.1$.

In Figure 7 we report a comparison between total flux as a function of the aperture radii for the two input targets (magnitude 16 and 18) and for the three images reconstructed with the PSF extracted from psf-star with

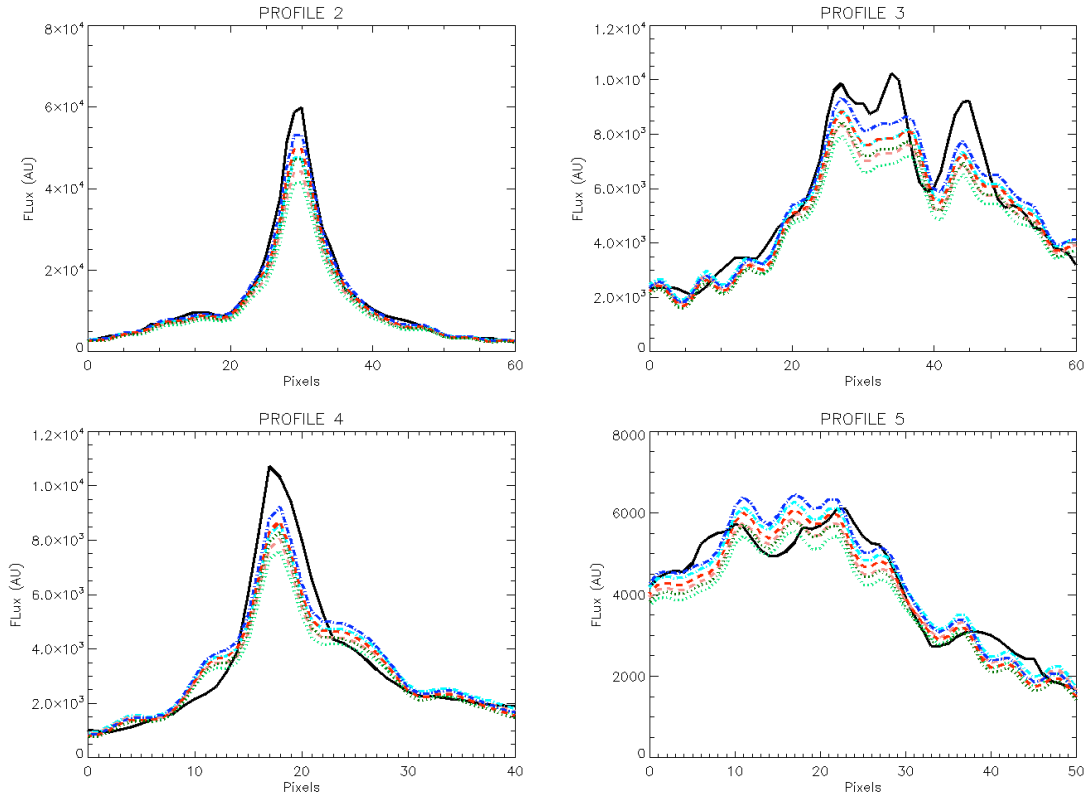


Figure 6. *The light distribution in 4 different profiles for the original galaxy (solid black line) and for reconstructed images (after 1000 iterations) obtained extracting the PSF from a psf-star of magnitude $K_s=14$ and using different radius (50 and 150 pixels) for the extraction region and different β (1.1, 1.15 and 1.2) for the Moffat function used to extrapolate the PSF to the full image domain. Line style and colors as in Figure 4. The location of the slices is shown in Figure 5. Profile 1 is not reported because very similar to profile 2.*

different magnitude, while a comparison of the light distribution in 4 different slices (as in Figure 6) is reported in Figure 8.

From the analysis of Figure 7 and 8, it is evident that while from the morphological point of view (Figure 8) the use of psf-star up to a magnitude of 18 is still acceptable, from the photometric point of view the use of psf-star fainter than $K_s \sim 16$ mag could cause considerable problems. For example, using a psf-star of $K_s=18$ mag we have a total flux overestimated by a factor 1.2 (both for the galaxy with $K_s=16$ and $K_s=18$, see Figure 7) corresponding to a photometric error of $\sim \Delta m=0.2$ mag.

5. SUMMARY AND CONCLUSION

In this document we report the results of our work on the simulation and reconstruction of LN images for a relatively distant galaxy at redshift ~ 1 . A total of three images at different equispaced hour angles have been simulated. Each single image has been obtained assuming an integration time of 60 minutes, for a total integration time of 3 hours. Using these simulated images, we obtained the final reconstructed images using the software package AIRY-LN. In order to test the performance of the method, we produced several reconstructed images obtained with different techniques. In particular we tested the quality of the reconstruction as function of the method used to extract the PSF from the image and the dependency on the psf star brightness.

Our general conclusions can be summarised as follows:

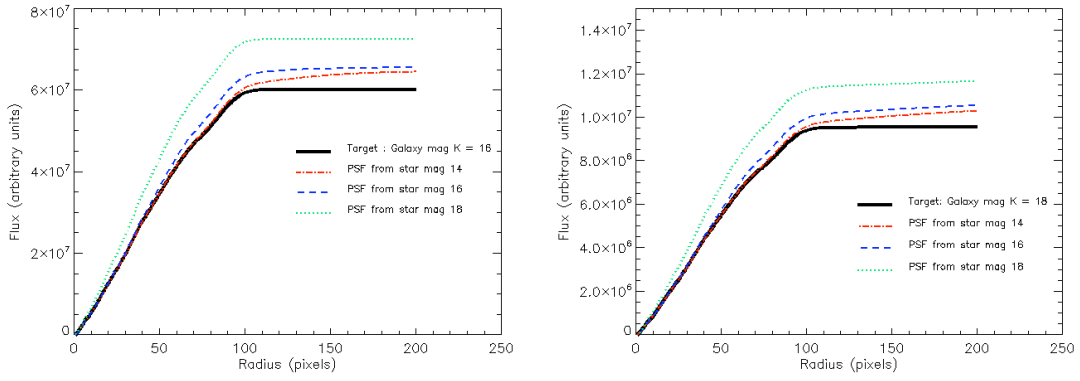


Figure 7. **Left:** The total flux of the original galaxy (magnitude $K_s=16$, solid black line) and the total flux calculated on the reconstructed images (after 1000 iterations) obtained extracting the PSF from a psf-star with magnitude $K_s=14$, 16 and 18 and extrapolating the PSF to the full image domain with a Moffat function with $\beta=1.1$. **Right:** The total flux of the original galaxy (magnitude $K_s=18$, solid black line) and the total flux calculated on the reconstructed images (after 1000 iterations) obtained extracting the PSF from a psf-star with magnitude $K_s=14$, 16 and 18 and extrapolating the PSF to the full image domain with a Moffat function with $\beta=1.1$.

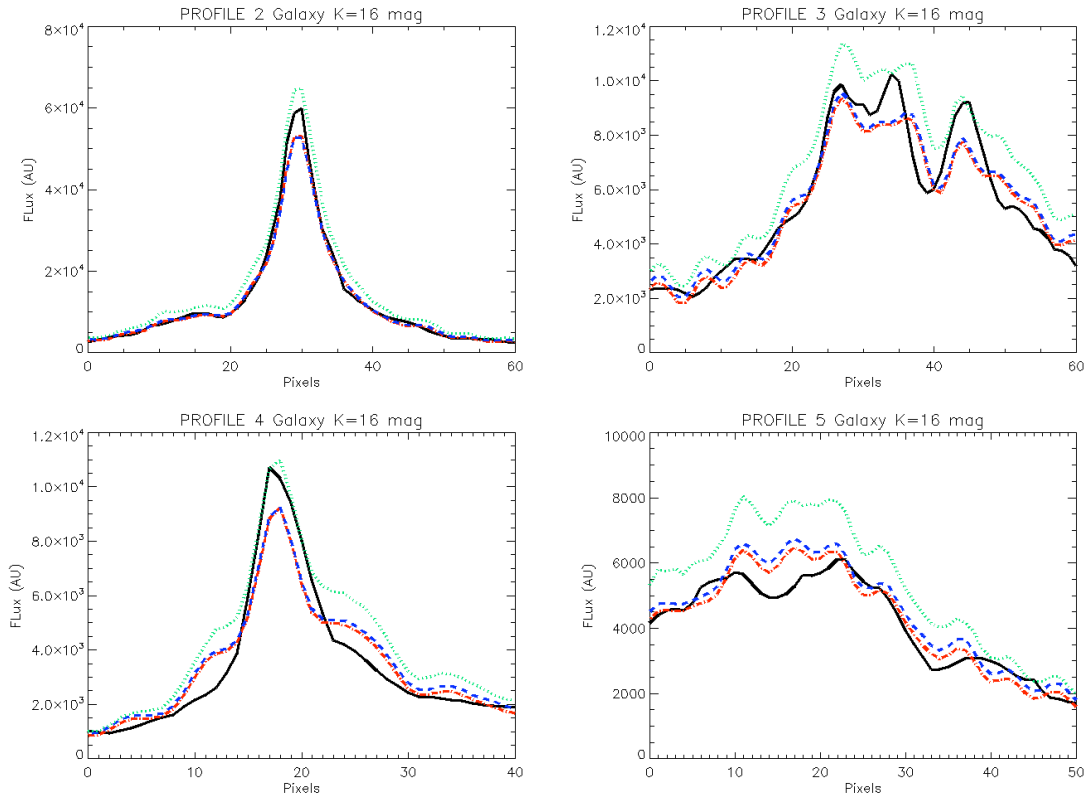


Figure 8. The light distribution in 4 different profiles for the original galaxy (solid black line) and for reconstructed images (after 1000 iterations) obtained extracting the PSF from a psf-star with magnitude $K_s=14$ (red dot dashed line), 16 (blue dashed line) and 18 (green dotted line). The location of the slices is shown in Figure 5.

- From the *Inverse Crime* technique (*i.e.* same PSF for generation and reconstruction of the images) we found that the reconstruction algorithm is fundamental to obtain a good reproduction of the original flux and morphology. In the non reconstructed images a large fraction of the galaxy flux is spread in the outer regions of the images, making the photometric accuracy very poor.
- Different reconstructions have been obtained extracting the PSF from a small region around the psf-star and extending it to the full image domain with two methods: adding a zero padding and extrapolating the PSF with a Moffat function in the form $I(r) = a/(b + r^2)^\beta$. While the zero padding technique, as expected, gives very poor results in terms of photometric accuracy, the extrapolation with a Moffat function with $\beta = 1.1$ gives very good results both in terms of photometric and morphological accuracy. However, more specific simulations, with different scientific targets and/or with different atmospheric conditions, are needed to obtain more robust results on the best fitting parameters for the PSF extrapolation.
- Finally we tested the dependency of the reconstructed image quality from the psf star brightness analyzing reconstruction obtained with psf-stars with different magnitudes. We found that while from the morphological point of view the use of psf-star up to a magnitude of 18 is still acceptable, from the photometric point of view the use of psf-star fainter than Ks ~ 16 mag could cause considerable problems, with an error of $\sim \Delta m = 0.2$ mag when a psf-star with Ks=18 mag is used.

REFERENCES

- [1] Hill, J.,M. and Salinari, P. *The Large Binocular Telescope Project SPIE 4837*, 15 (2003)
- [2] Herbst, T.M., Ragazzoni, R., Andersen, D., Boehnhardt, H., Bizenberger, P., Eckart, A., Gaessler, W., Rix, H.W., Rohloff, R.R., Salinari, P., Soci, R., Straubmeier, C., Xu, W., *LINC-NIRVANA: a Fizeau Beam Combiner for the Large Binocular Telescope, SPIE*, vol. 4838, p. 456, (2003)
- [3] Bizenberger, P., Diolaiti, E., Egner, S., Herbst, T., M., Ragazzoni, R., Reymann, D. and Xu, W. *LINC-NIRVANA: optical design of an interferometric imaging camera SPIE 6269,11* (2006)
- [4] Arcidiacono, C., Diolaiti, E., Tordi, M., Ragazzoni, R., Farinato, J., Vernet, E., and Marchetti, E., *Layer-Oriented Simulation Tool, Appl. Optics*, vol. 43, issue 22, (2004)
- [5] Ragazzoni, R., Diolaiti, E., Farinato, J., Fedrigo, E., Marchetti, E., Tordi, M., and Kirkman, D., *Multiple field of view layer-oriented adaptive optics, A&A*, 396, pp. 731-744, (2002)
- [6] Fini, L., Carbillet, M. and Riccardi, A., *The CAOS Application Builder, ASP Conf. Ser. ADASS X*, eds F. A. Primini & F. R. Harnden, 253 (2001)
- [7] Correia, S., Carbillet, M., Boccacci, P., Bertero, M., and Fini, L., *Restoration of inteferometric images - I. The software package AIRY, A&A*, 387, pp. 733-743, (2002)
- [8] Desiderà, G., La Camera, A., Boccacci, P., Bertero, M. and Carbillet M., *AIRY-LN: an ad-hoc numerical tool for deconvolution of images from the LBT instrument LINC-NIRVANA SPIE 7013, 701340* (2008)
- [9] Bertero, M., and Boccacci, P., *Application of the OS-EM method to the restoration of the LBT images, A&AS*, 144, pp. 181-186, (2000)
- [10] Hudson, H. M., and Larkin, R. S., *Accelerated image reconstruction using ordered subsets of projected data, IEEE Trans. Med. Imag.*, vol. 13, pp. 601609, (1994)
- [11] La Camera, A., Desiderà, G., Arcidiacono, A., Boccacci, P., Bertero, M., *Advances in the reconstruction of LBT LINC-NIRVANA images, A&A*, 471, pp. 1091-1097, (2007)